The Compact Root Architecture 2 systemic pathway is required for the repression of cytokinins and miR399 accumulation in Medicago truncatula N-limited plants

Journal of Experimental Botany

Argirò, Luca; Laffont, Carole; Moreau, Corentin; Moreau, Carol; Su, Yangyang et al

https://doi.org/10.1093/jxb/erae281

Journal of Experimental Botany, Vol. 75, No. 18 pp. 5667–5680, 2024
https://doi.org/10.1093/jxb/erae281 Advance Access Publication 28 June 2024

RESEARCH PAPER

The Compact Root Architecture 2 systemic pathway is required for the repression of cytokinins and miR399 accumulation in *Medicago truncatula* N-limited plants

Luca Argirò[1,†], Carole Laffont[1,†], Corentin Moreau[1,†], Carol Moreau[1,†], Yangyang Su[1,†], Marjorie Pervent[2], Hugues Parrinello[3], Thomas Blein[1], Wouter Kohlen[4], Marc Lepetit[5], and Florian Frugier[1,*]

[1] Institute of Plant Sciences – Paris Saclay (IPS2), University of Paris-Saclay, CNRS, University of Paris-Cité, INRAE, Univ Evry, Bat 630, Avenue des Sciences, 91190 Gif-sur-Yvette, France
[2] Plant Health Institute of Montpellier (PHIM), INRAE, SupAgro, University of Montpellier, CIRAD, IRD, Campus de Baillarguet, 34398 Montpellier, France
[3] MGX-Montpellier GenomiX, University of Montpellier, CNRS, INSERM, 34398 Montpellier, France
[4] Laboratory of Cell and Developmental Biology, Department of Plant Sciences, Wageningen University & Research, 6708 PB Wageningen, The Netherlands
[5] Institute of Sophia Agrobiotech (ISA), INRAE, Université Côte d'Azur, CNRS, 06903 Sophia-Antipolis, France

[†] These authors contributed equally to this work.
* Correspondence: florian.frugier@cnrs.fr

Received 14 March 2024; Editorial decision 18 June 2024; Accepted 27 June 2024

Editor: Miriam Gifford, University of Warwick, UK

Abstract

Legume plants can acquire mineral nitrogen (N) either through their roots or via a symbiotic interaction with N-fixing rhizobia bacteria housed in root nodules. To identify shoot-to-root systemic signals acting in *Medicago truncatula* plants at N deficit or N satiety, plants were grown in a split-root experimental design in which either high or low N was provided to half of the root system, allowing the analysis of systemic pathways independently of any local N response. Among the plant hormone families analyzed, the cytokinin *trans*-zeatin accumulated in plants at N satiety. Cytokinin application by petiole feeding led to inhibition of both root growth and nodulation. In addition, an exhaustive analysis of miRNAs revealed that miR2111 accumulates systemically under N deficit in both shoots and non-treated distant roots, whereas a miRNA related to inorganic phosphate (Pi) acquisition, miR399, accumulates in plants grown under N satiety. These two accumulation patterns are dependent on Compact Root Architecture 2 (CRA2), a receptor required for C-terminally Encoded Peptide (CEP) signaling. Constitutive ectopic expression of miR399 reduced nodule numbers and root biomass depending on Pi availability, suggesting that the miR399-dependent Pi-acquisition regulatory module controlled by N availability affects the development of the whole legume plant root system.

Keywords: CEP peptide, CLE peptide, CRA2 receptor, cytokinin, legume, microRNA, miR399, nitrogen-fixing symbiotic root nodulation, phosphate.

Introduction

Plants use various mineral nutrient sources to ensure their growth, notably nitrogen (N), whose acquisition is mediated through the root system. As the distribution of mineral N in soils is heterogeneous and fluctuates, plants have evolved mechanisms to perceive its local availability and modulate their root system architecture accordingly. In addition, systemic regulatory pathways, acting at the whole-plant level between shoots and roots, allow the adjustment of plant growth and metabolism to nutrient availability (de Kroon *et al.*, 2009; Gautrat *et al.*, 2021; Lepetit and Brouquisse, 2023; Valmas *et al.*, 2023).

In addition to mineral N acquisition by roots, many legume plants use an additional strategy to acquire N. When mineral N is limited and compatible soil bacteria (collectively named rhizobia) are present in the rhizosphere, root nodules can be formed (Roy *et al.*, 2020). Within the root nodules, N-fixing rhizobia are housed intracellularly and produce ammonium in exchange for plant-derived photoassimilates. This ammonium can be used by the host plant to fuel its N metabolism and, thus, its growth in N-limited soils.

In *Medicago truncatula*, two types of peptide hormones regulating nodulation have been shown to contribute to systemic root-to-shoot signaling depending on N availability in soils. First, the production of CEP (C-terminally Encoded Peptide) signaling peptides is induced in roots grown under low-N conditions. These peptides are transported through the xylem to the shoot, where they activate the CRA2 (Compact Root Architecture 2) receptor, which in turn stimulates nodulation in roots (Imin *et al.*, 2013; Mohd-Radzman *et al.*, 2016; Laffont *et al.*, 2019). CRA2 is orthologous to CEPR1 (CEP RECEPTOR 1) in *Arabidopsis thaliana* (Tabata *et al.*, 2014). CEPR1 perceives CEP signaling peptides that are similarly produced in conditions of low N availability. CEP peptides act as root-to-shoot signals to systemically promote N-acquisition. Second, the production of a *M. truncatula*-specific CLE (CLAVATA3-Like/Embryo surrounding region-related) signaling peptide, MtCLE35, is induced in roots grown in high N, similar to that previously reported in other legumes such as *Lotus japonicus* and soybean (Okamoto *et al.*, 2009; Reid *et al.*, 2011; Gautrat *et al.*, 2021; Moreau *et al.*, 2021). This CLE peptide acts in shoots through the SUNN (Supernumerary Nodules) receptor to repress nodulation. In addition, the expression of *MtCLE35* is up-regulated in roots by rhizobia to similarly act systemically through the SUNN receptor to repress further nodule initiation.

In the shoot, the CEP/CRA2 and CLE/SUNN pathways converge to antagonistically regulate the microRNA miR2111. miR2111 moves from the shoot to the root through the phloem, and in roots represses the accumulation of transcripts of *TML* (*Too Much Love*). *TML* genes encode negative regulators of nodulation (Gautrat *et al.*, 2019). By repressing the repressors, CEP/CRA2 stimulates nodule formation. On the other hand, CLE/SUNN blocks the miRNA-mediated negative regulation of *TMLs* and, as such, represses nodulation (Gautrat *et al.*, 2020, 2021).

In addition to these signaling peptides, cytokinins were shown to act as another systemic shoot-to-root signal in *L. japonicus*, negatively regulating nodulation in response to rhizobia (Sasaki *et al.*, 2014). Interestingly, in *A. thaliana*, a non-nodulating plant, cytokinins also act as a systemic shoot-to-root signal to regulate the root system architecture depending on the whole-plant N status (Poitout *et al.*, 2018; Gautrat *et al.*, 2021). Cytokinins are also involved in root-to-shoot signaling to modulate shoot metabolism and growth in plants at N satiety (Sakakibara, 2021). Finally, at a later nodulation stage, is it likely that other systemic regulations exist to modulate the N-fixation activity in differentiated nodules depending on the plant's N demand (Pervent *et al.*, 2021).

The whole-plant N status is not the only nutritional factor determining the competence of legume roots to form nodules. In addition to high N, low inorganic phosphate (Pi) availability inhibits nodulation, notably in *M. truncatula* (Sulieman *et al.* 2013). The microRNA miR399 is one of the key regulators of the response to Pi availability in non-symbiotic plants. Indeed, this miRNA, acting systemically from shoots to roots, negatively regulates the accumulation of *PHO2* (*Phosphate 2*) transcripts in roots. *PHO2* encodes an F-box protein that mediates the degradation of the PHO1 (Phosphate 1) Pi transporters and, therefore, acts as a negative regulator of Pi acquisition (Branscheid *et al.*, 2010; Prathap *et al.*, 2022). In *M. truncatula*, a systemic function of the miR399/PHO2 module on Pi acquisition was similarly demonstrated in relation to another root endosymbiosis with arbuscular mycorrhizal fungi. However, miR399 overexpression was not sufficient to enhance mycorrhizal colonization, suggesting that miR399 is induced to fine-tune *MtPHO2* activity when symbiotic Pi uptake is activated in mycorrhizal roots, but it is not directly involved in the regulation of mycorrhizal colonization (Branscheid *et al.*, 2010).

To identify novel hormonal and miRNA shoot-to-root systemic effectors mediating the N status in a legume plant, *M. truncatula* was grown in the same split-root experimental system as that previously described by Pervent *et al.* (2021). We used this specific experimental system to discriminate between local root and systemic responses to N availability. Half of the plant's root system was supplied with either high or low mineral N, whereas the other half received no N. As both hormones and miRNAs were shown to act as systemic signals, we analyzed their differential accumulation simultaneously in shoots and in the half of the root system that received no N treatment. As these regulations occur in the absence of local N, they must result from systemic signaling. The identification of the previously characterized miR2111 systemic signal allowed validation that the strategy used was effective to identify shoot-to-root signals linked to N availability. Additional hormonal and/or miRNA systemic signals with a congruent

accumulation pattern in both shoots and non-treated distant roots were then searched for. The analysis of different plant hormones revealed that, among all the hormones tested, only *trans*-zeatin (*tZ*) showed a similar increase in content in shoots and roots of plants grown under N satiety. In agreement with this N-driven accumulation pattern, cytokinins applied to shoots by a petiole-feeding strategy inhibited both root development and nodulation. In addition, an exhaustive expression analysis of miRNAs revealed that miR399 accumulated in both systemic shoots and roots of plants grown under N satiety. Accordingly, miR399 overexpression inhibited both root growth and nodule formation, suggesting the existence of an N-availability-driven systemic regulation of Pi accumulation to modulate root and nodule development.

Materials and methods

Biological material, plant growth conditions and treatments

The *M. truncatula* Jemalong A17 wild-type genotype and the *cra2-11* mutant derived from this genotype (Laffont *et al.*, 2019) were used in this study. Seeds were scarified by immersion in pure sulfuric acid for 3 min, washed six times with water, and then sterilized for 20 min in Bayrochlore (3.75 g l^{-1}, Bayrol, Chlorofix). Seeds were washed again, transferred on to water/BactoAgar plates (Difco), stratified for 4 d in the dark at 4 °C, and then germinated at 24 °C in the dark overnight.

Split-root experimental N-satiety (NS) versus N-deficit (ND) conditions were set up as described by Pervent *et al.* (2021). Plants were grown in a growth chamber with a 16 h photoperiod and a light intensity of 250 µmol m^{-2} s^{-1}, a relative humidity of 70%, and temperatures of 22 °C day/20 °C night, in hydroponic tanks containing a vigorously aerated 'HY' basal nutrient solution (1 mM KH_2PO_4, 1 mM $MgSO_4$, 0.25 mM $CaCl_2$, 0.25 mM K_2SO_4, 50 µM KCl, 30 µM H_3BO_3, 5 µM $MnSO_4$, 1 µM $ZnSO_4$, 1 µM $CuSO_4$, 0.7 µM $(NH^4)_6Mo_7O_{24}$, and 100 µM Na-Fe-EDTA; pH adjusted to 5.8 with KOH) supplemented with 0.5 mM KNO_3 as the sole mineral N source, which was renewed every 4 d. After 1 week, the primary root tips of plantlets were cut to promote the branching of the root system. The root systems of 3-week-old plants were separated into two parts and grown in a split-root system. Four days before harvest, the differential local N treatments were applied using HY solution supplemented with high mineral N (10 mM NH_4NO_3) or low mineral N (0.05 mM KNO_3), whereas systemic root compartments were supplied with HY solution without added mineral N (Fig. 1A). Four-week-old plants were harvested in the middle of the day.

For the investigation of nodulation kinetics, germinated seedlings were grown *in vitro* on a growth culture paper (Mega International, https://mega-international.com/) in vertical 1.5% BactoAgar plates containing Fahraeus medium (Fahraeus, 1957). Plates were placed in a growth chamber with a 16 h photoperiod, a light intensity of 150 µmol m^{-2} s^{-1}, and a temperature of 24 °C. *Sinorhizobium medicae* WSM419 strain was used to nodulate *M. truncatula* plants. Bacteria were grown overnight at 30 °C on a yeast extract broth medium, and roots were then inoculated with a bacterial suspension at OD_{600nm}=0.05. Samples were harvested at 0, 1, 4, 8, and 15 days post inoculation (dpi) with rhizobia.

For experiments aiming to test the impact of Pi availability on gene expression, plants were watered with Fahraeus medium (Fahraeus, 1957) containing 7.5 mM NH_4NO_3 and either 1.5 mM, 100 µM, or 20 µM KH_2PO_4. Samples were harvested at 14 d post germination.

For experiments aiming to test the impact of *MtCEP1* or *MtCLE35* overexpression on gene expression, transformed plants were transferred into pots containing a sand:perlite 1:3 mixture, which were placed in a growth chamber with a 16 h photoperiod, a light intensity of 150 µmol m^{-2} s^{-1}, a temperature of 24 °C, and relative humidity of 70%. Plants were watered with Fahraeus medium with either low N (–N; KNO_3 0.5 mM) or high N (+N; NH_4NO_3 10 mM) to generate, respectively, a whole-plant ND or NS.

For experiments aiming to test the impact of Pi availability on nodulation, plants were watered with Fahraeus medium containing 0.2 mM KNO_3 and either 1.5 mM, 100 µM, or 20 µM KH_2PO_4. Plants were inoculated with rhizobia as described above, and the number of nodules and root dry weight were measured at 14 dpi.

For experiments aiming to test the impact of miR399 overexpression on nodulation, plants were watered with Fahraeus medium containing 0.2 mM KNO_3 and either 1.5 mM or 100 µM KH_2PO_4. Plants were inoculated with rhizobia as described above, and the nodule number and root dry weight were measured at 14 dpi.

For petiole-feeding assays, plants were grown in the same sand:perlite mixture and conditions as those described above, and watered for 1 week with 'i' medium (Blondon, 1964) supplemented with N (KNO_3 1 mM), and then watered with low-N 'i' medium. At 28 d after germination, plants were inoculated with the *S. medicae* WSM419 strain, and at the same time a leaf was cut and the corresponding petiole placed into an Eppendorf tube with the cytokinin benzylaminopurine (BAP) (Sigma-Aldrich) at 10^{-5} M. Feeding was maintained over 14 d, with the hormonal solution being refilled every 3 d. Nodule number and root dry weight were measured at 14 dpi.

Hormone quantifications

For the extraction of plant growth regulators from *M. truncatula*, ~20 mg of snap-frozen plant material was used per sample and extracted as previously described (Schiessl *et al.* 2019; Gühl *et al.*, 2021) with the addition of abscisic acid (ABA), salicylic acid (SA), jasmonic acid (JA), JA-isoleucine (JA-Ile), and 12-oxo-phytodienoic acid (OPDA) stable isotope-labeled internal standards (Supplementary Table S1).

Sample residues were dissolved in 100 µl of acetonitrile/water (20:80, v/v) for the acid fraction [indole acetic acid (IAA), SA, JA, ABA] and MeOH/water (20:80, v/v) for the cytokinin fraction [isopentenyl adenine (iP), *tZ*, *cis*-zeatin (*cZ*), and their respective riboside derivatives (iPR, *tZR*, *cZR*)], and filtered through a 0.45 mm Minisart SRP4 filter (Sartorius, Göttingen, Germany). Analyses of plant growth regulators was performed by comparing retention times and mass transitions with those of unlabeled standards (Supplementary Table S1) using a Waters XevoTQs mass spectrometer equipped with an electrospray ionization source coupled to an Acquity UPLC system (Waters, Milford, USA), as previously described (Schiessl *et al.*, 2019; Gühl *et al.*, 2021). Multiple reaction monitoring (MRM) transitions, cone voltage, and collision energy selected for compound identification and quantification are shown in Supplementary Table S1. To determine sample concentrations, a 10-point calibration curve was constructed for each compound ranging from 1 µM to 190 pM, and each dilution also contained a known amount of an appropriate deuterium-labeled internal standard.

RNA extraction, library preparation, and sequencing

For each condition, three biological samples were harvested and analyzed. Each biological sample was a pool of three plants grown in parallel. Total RNAs were extracted using the miRNeasy mini kit (Qiagen). The total RNAs were quantified using a Fragment Analyzer with the Standard Sensitivity RNA Analysis kit (Agilent Technologies). Small RNA-seq libraries were prepared using the NEXTFLEX Small RNA-seq kit v3 (PerkinElmer) following the manufacturer's instructions. Briefly, a 3′ adenylated adapter was ligated to the 3′ end of 320 ng of RNA and purified to remove the excess of 3′ adapter. A 5′ adapter was ligated to the 5′ end of the 3′ ligated microRNA. The resulting construction was purified to

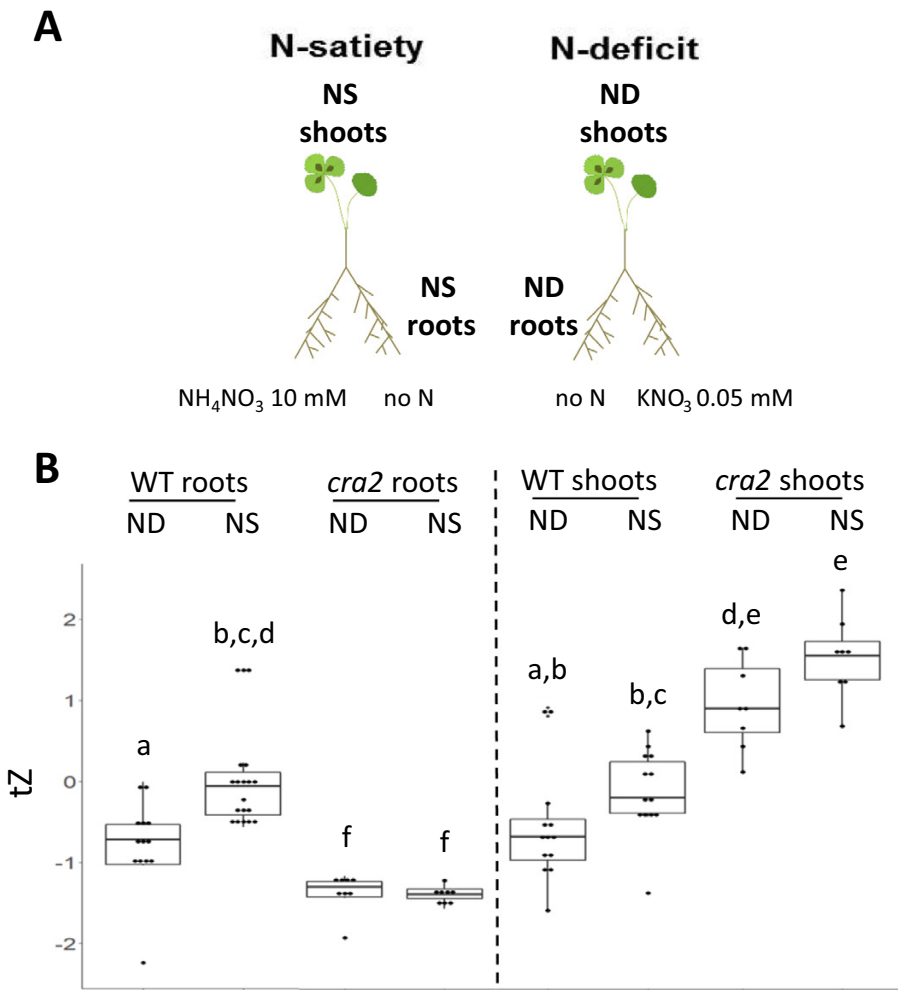

Fig. 1. The accumulation of the cytokinin *trans*-zeatin (*tZ*) depending on the plant N status requires the CRA2 pathway. (A) Experimental design of the split-root assay used to analyze the systemic shoot and root responses of *Medicago truncatula* to N availability. Half the root system of plants was locally treated with either low N (KNO_3 0.5 mM) or high N (NH_4NO_3 10 mM), to generate, respectively, a whole-plant N deficit (ND) or a whole-plant N satiety (NS). To specifically study systemic responses to ND or NS, only shoots and the other half root system (grown without N) were used for further analyses. As systemic signals result from N assimilation, they are independent of the local N source used (NO_3^-, or NH_4^+ and NO_3^-). (B) Differential accumulation of *tZ* in wild-type (WT) or *cra2* mutant ND versus NS plants. Raw data were quantified in pmol g^{-1} of fresh weight of shoots and/or roots, and data shown are centered reduced around the mean to allow direct comparisons between samples. Letters above the plots indicate significant differences based on a Kruskal–Wallis test (α=0.05). Center lines show the medians of three (n=10 plants for each replicate and condition) independent biological replicates; box limits indicate the 25th and 75th percentiles; whiskers extend to 1.5 times the interquartile range from the 25th and 75th percentiles; individual data points are represented by dots.

remove the excess of 5′ adapter. The 5′ and 3′ ligated microRNAs then underwent reverse transcription using a Mo-MuLV reverse transcriptase and a primer complementary to the 3′ adapter. The resulting cDNAs were PCR amplified for 17 cycles using a pair of uniquely barcoded primers. The resulting barcoded library was size selected (137–187 bp) using a Pippin HT (SAGE Science) with a 3% agarose cassette (#HTG3004). The size distribution of the resulting libraries was monitored using a Fragment Analyzer with the High Sensitivity NGS kit (Agilent Technologies), and the libraries were quantified using the KAPA Library quantification kit (Roche). Finally, the libraries were denatured with NaOH, neutralized with Tris–HCl, and diluted to 300 pM. Clustering and sequencing were performed on a NovaSeq 6000 (Illumina, San Diego, CA, USA) using the single-end 100 nt protocol on two lanes of a SP flow cell.

Small RNA sequencing data analysis

Image analyses and base calling were performed using the NovaSeq Control Software and the Real-Time Analysis component (Illumina). Demultiplexing and trimming were performed using Illumina's conversion software (bcl2fastq 2.20). The quality of the raw data was assessed using FastQC (v0.11.8) from the Babraham Institute and the Illumina software SAV (Sequencing Analysis Viewer). FastqScreen (v0.14.0) was used to identify potential contamination. The raw reads were trimmed using Cutadapt (v2.7) (Martin, 2011) to remove the sequencing adapter (TGGAATTCTCGGGTGCCAAGG) at the 3′ end. Additionally, four bases were trimmed from the 5′ end and the 3′ end of the reads as described in the manual of the NEXTFLEX Small RNA-Seq Kit v3 (Perkin-Elmer).

The amount of each mature miRNA was computed as the number of mature reads exactly corresponding to the mature sequence. The miRNA mature sequences were retrieved from miRBase (v22, https://www.mirbase.org/) and the MirMed databases (https://medicago.toulouse.inra.fr//Mt/RNA/MIRMED/NR120620_PAPER/smallA/cgi-bin/learn.cgi; Formey *et al.*, 2014). A differential miRNA accumulation analysis was performed with DEseq2 (v1.16.1) (Love *et al.*, 2014) using a linear model. Low counts were discarded using DESeq2 independent filtering with default parameters, and raw *P* values were adjusted with the Bonferroni method.

The quality of the small RNA libraries was evaluated using a principal component analysis (PCA) approach (Supplementary Fig. S1), which revealed first that biological replicates of each organ (shoot or root) grouped together, and second that the two genotypes (wild-type and *cra2* mutant) were clearly separated, indicating the appropriate quality of the samples.

Heatmaps were generated using R (https://www.r-project.org/) and the Rstudio software (http://www.rstudio.com/). A mean-centered normalization was applied on raw data (*P* value <0.05), which were then clustered using a *K*-means method.

Quantitative reverse transcription–PCR analysis

The Quick-RNA MiniPrep Kit (Ozyme) was used to perform long and small RNA extractions. Extracted RNAs were then treated with DNase1 RNase-free (Thermo Fisher), following the manufacturer's instructions. cDNAs were obtained using the SuperScript III Reverse Transcriptase (200 U ml^{-1}), following the manufacturer's instructions. A stem-loop reverse transcription (RT) was performed to amplify specifically mature miRNAs after including dedicated adapters (listed in Supplementary Table S2), as described by Gautrat *et al.* (2020). Two independent cDNA samples were generated from each RNA sample as technical replicates.

Gene expression was then analyzed by quantitative RT–PCR (qRT–PCR) on a LightCycler96 apparatus (Roche), using the Light Cycler 480 SYBR Green I Master mix (Roche) and dedicated specific primers to amplify each gene of interest (listed in Supplementary Table S2). Forty-five amplification cycles were performed (15 s at 95 °C, 15 s at 60 °C, 15 s at 72 °C), and a final fusion curve from 60 °C to 95 °C was used to assess the amplification specificity. Amplicons were independently sequenced to confirm the specificity of the PCR amplification. Primer efficiency was systematically tested, and only primers with an efficiency >90% were retained. Gene expression was normalized using two different reference genes, *MtActin11* and *MtRNA Binding Protein 1* (*MtRBP1*); miRNA accumulation was normalized using the miR162 mature miRNA (the primers used are listed in Supplementary Table S2).

Cloning procedures and root transformation

The CEP1 overexpression plasmid and its associated control were generated as described in Imin *et al.* (2013). The CLE35 overexpression plasmid and its associated control were generated as described in Moreau *et al.* (2021). The p35S:miR399c construct was generated using a Golden Gate strategy and vectors described by Engler and Marillonnet (2014). The miR399c precursor (MtrunA17Chr8g0379333; *M. truncatula* genome v5; https://medicago.toulouse.inra.fr/MtrunA17r5.0-ANR/) was amplified by PCR using the primers indicated in Supplementary Table S2. This PCR amplicon was inserted into the L1 Golden Gate vector (EC47811, ampicillin resistant) together with the 35S promoter (EC15058) and the 35S terminator (EC41414) cassette. After validation by sequencing of the L1 vector, an L2 vector (EC50507) was produced by adding a pNOS:Kanamycin cassette (EC15029) to allow plant selection on kanamycin. A β-glucuronidase (GUS) control vector was generated with the same strategy, using the GUS cassette (EC75111).

Final binary vectors were transformed into the *Agrobacterium rhizogenes* Arqua1 strain to generate 'composite plants' with wild-type shoots and transformed roots, with each transgenic root thus being the result of independent genetic transformation events, selected for 2 weeks on Fahraeus medium with kanamycin (25 mg ml^{-1}), following the protocol described by Boisson-Dernier *et al.* (2001).

Statistical analyses

Statistical analyses were performed with R (https://www.r-project.org/) and the Rstudio software (http://www.rstudio.com/), using a Kruskal–Wallis test or a Mann–Whitney U test when more than two or only two conditions, respectively, were compared. Boxplots were generated using tools available at http://shiny.chemgrid.org/boxplotr/.

Results

The regulation of *trans*-zeatin cytokinin systemic accumulation depending on the plant N status requires the CRA2 pathway

To identify hormones that accumulate to a similar extent in both shoots and roots at a distance from the low-N or high-N application, plants were grown in split-root systems with either low-N (KNO_3 0.05 mM) or high-N (NH_4NO_3 10 mM) provision on half of their root system, and no mineral N supplied to the other half (Fig. 1A). This allowed analysis in parallel of the pattern of accumulation of hormones in the shoots and roots of plants in ND or NS that were not in direct contact with the N treatment. Five families of plant hormones were simultaneously analyzed using MRM-UPLC-MS/MS. These five families comprised auxin (IAA), cytokinins (*t*Z, *c*Z, and iP, and their riboside derivatives), SA, jasmonates (JA, JA-Ile), and ABA (Schiessl *et al.*, 2019; Gühl *et al.*, 2021) (Fig. 1; Supplementary Fig. S2). The criteria used for selecting candidate shoot-to-root systemic signals was their antagonistic accumulation patterns between ND shoots/systemic roots and NS shoots/systemic roots. None of the hormonal species analyzed fell into this category. Nevertheless, the bioactive cytokinin *t*Z accumulated more in the roots of plants grown in NS compared with ND and showed a similar, although not significant, trend in NS shoots (Fig. 1B). No difference was detected in the relative levels of auxin, SA, and any of the other cytokinins analyzed when comparing shoots and systemic roots grown under our experimental conditions (Supplementary Fig. S2). JA and ABA were detected at relatively low concentrations in all root samples compared with shoots, and showed greater accumulation in ND shoots compared with NS shoots (Supplementary Fig. S2). JA-Ile showed a similar, although not significant, trend compared with JA. However, ABA and JA were not considered *bona fide* systemic signals as only low concentrations of these hormones were detected in roots, and no congruent differences were observed between systemic roots of ND and NS plants relative to the corresponding shoots.

As CRA2 is key for regulating systemic responses related to N availability, the accumulation of the cytokinin *t*Z was then analyzed in the *cra2* mutant using the same split-root

experimental design (Fig. 1A). This experiment revealed that the CRA2 signaling pathway was necessary for *tZ* differential accumulation in NS versus ND plants (Fig. 1B).

To evaluate a possible systemic role of cytokinins in regulating root growth and/or nodulation, we used a petiole-feeding assay to test the effect of a local shoot application of cytokinins on these developmental phenotypes. Cytokinins applied to the shoot inhibited both root nodulation and root growth (Fig. 2A, B). This result suggests that, under high-N nodulation-inhibiting conditions, cytokinins could act as a shoot-to-root systemic signal inhibiting root growth and, either directly or indirectly, nodule formation.

miR399 systemically accumulates in plants at N satiety

Shoot-to-root systemic regulations have been reported to involve not only mobile hormonal signals but also a subset of miRNAs (Branscheid *et al.*, 2010; Gautrat *et al.*, 2020; Maizel *et al.*, 2020). The same split-root experimental design (Fig. 1A) was therefore also used to identify candidate shoot-to-root systemic miRNAs that would accumulate in a similar fashion in both shoots and roots of plants at ND or NS, independent of a local N response. Small RNA libraries were generated and sequenced, leading to the detection of 326 miRNA species that were previously annotated and deposited in the MiRBase and/or MirMed databases (Kozomara *et al.*, 2019; Formey *et al.*, 2014) (Supplementary Table S3A). Among these, 106 miRNA isoforms were differentially expressed in shoots and/or roots of ND or NS plants ($P<0.05$) (Supplementary Table S3B; Fig. 3A). This number was reduced to 47 when taking into account a $|\log_2$ fold change$|$ >1 threshold (as indicated by the red and green colors in Supplementary Table S3). Focusing on annotated miRNAs, 40 showed opposite accumulation patterns between shoots and non-treated systemic roots (Supplementary Table S3B), corresponding first to miRNAs accumulating in shoots of NS plants and in roots of ND plants (e.g. miR156, miR166, miR168, miR169 and some isoforms of miR396), and second, to miRNAs having the alternative accumulation pattern, that is, accumulating systemically in roots of NS plants and in shoots of ND plants (e.g. miR164, miR319, other isoforms of miR396, and miR398). In contrast, Venn analyses identified five other miRNA isoforms that accumulated simultaneously in both shoots and roots of ND or NS plants (Fig. 3B; Supplementary Table S3C). First, in line with previous reports, the miR2111 family (four isoforms) accumulated in both shoots and systemic roots of plants under ND, highlighting the role of miR2111 as a systemic signal promoting nodule formation under low N (Gautrat *et al.*, 2020; Moreau *et al.*, 2021). Second, in plants under NS, a single miRNA isoform belonging to the miR399 family was detected to accumulate simultaneously in both shoots and roots (Fig. 3A; Supplementary Table S3C). This finding suggests that miR399 may act as a shoot-to-root systemic effector in NS plants. Overall, although several miRNAs showed a differential accumulation pattern between shoots and roots of ND or NS plants, only miR2111 and miR399 accumulated congruently in both shoots and roots of ND or NS plants, respectively, consistent with a putative systemic shoot-to-root function.

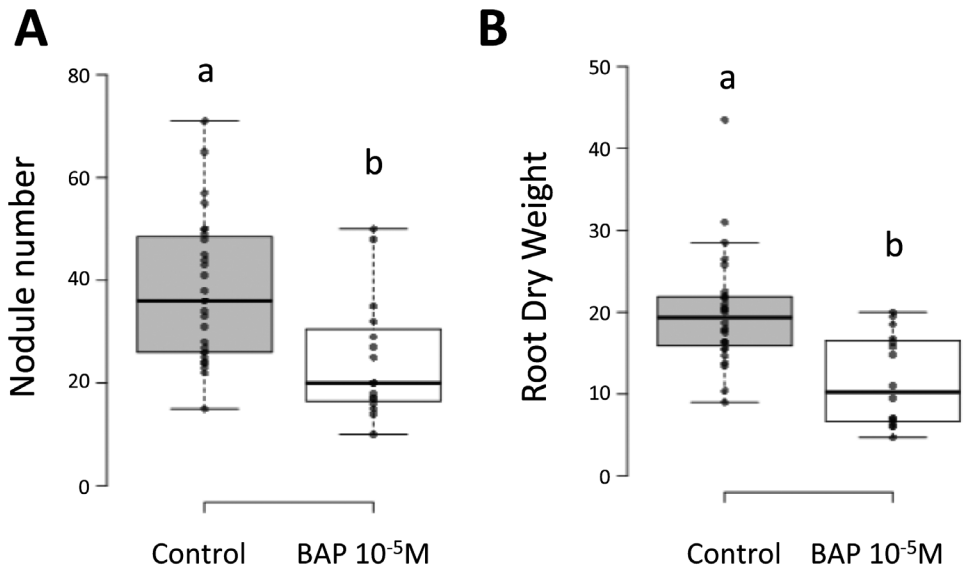

Fig. 2. Cytokinin inhibits nodulation and root growth when applied to shoots by petiole feeding. (A, B) Quantification of nodule number (A) and root dry weight (B) in response to petiole feeding with the cytokinin benzylaminopurine (BAP 10^{-5} M), compared with a mock (water) control. Petiole feeding was used to allow application specifically to shoots, to analyze its distant (systemic) effect on roots and nodules. Center lines show the medians of two (n>25 plants for each replicate and condition) independent biological replicates; box limits indicate the 25th and 75th percentiles; whiskers extend to 1.5 times the interquartile range from the 25th and 75th percentiles; individual data points are represented by dots. Letters above the plots indicate significant differences based on a Mann–Whitney U test (α=0.05).

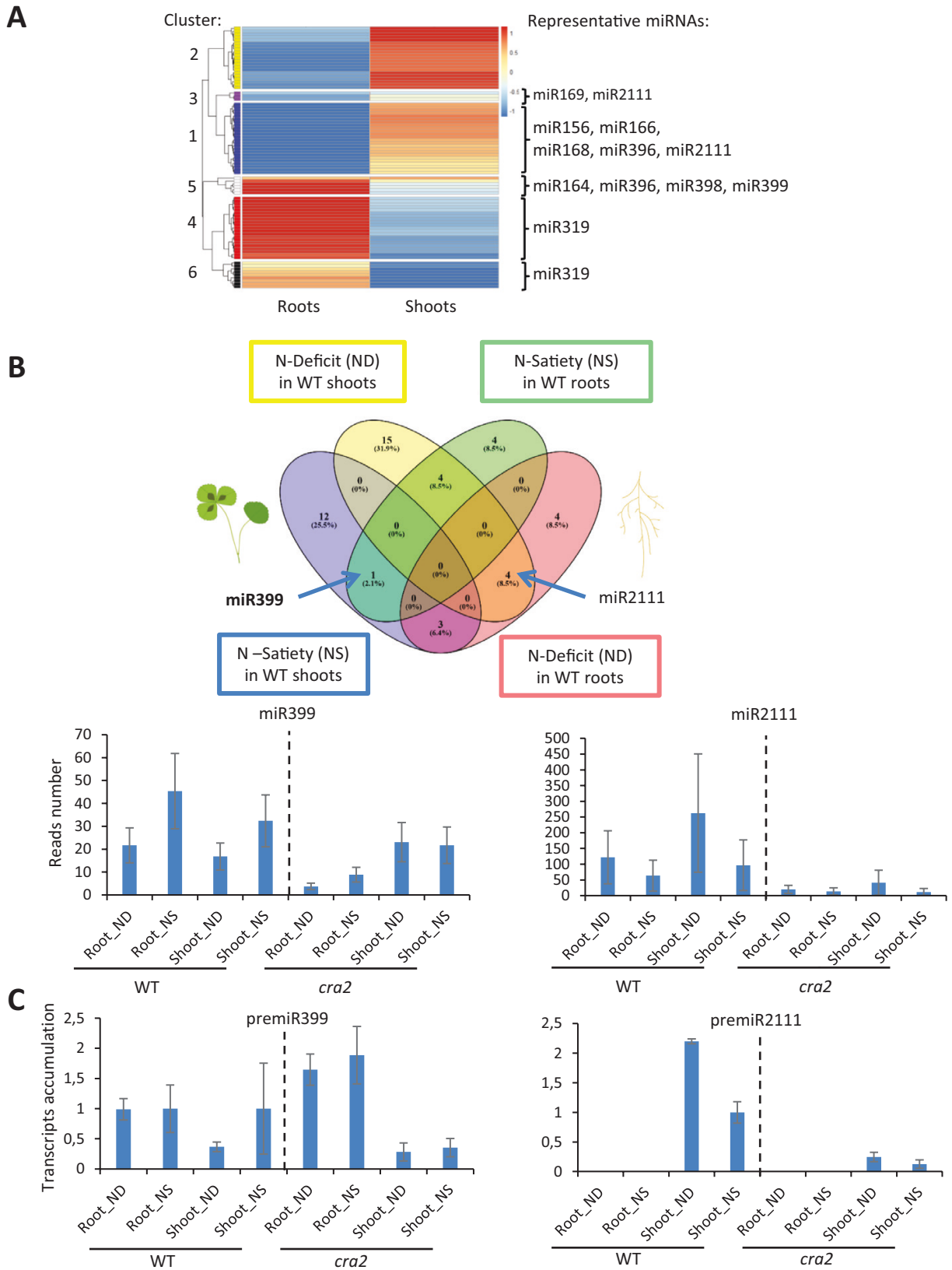

Fig. 3. Small RNA-seq analyses highlight candidate systemic miRNAs differentially regulated through the CRA2 pathway in plants at N deficit (ND) or N satiety (NS) in both shoots and roots. Plants were grown in the split-root experimental design described in Fig. 1A. (A). Heat map of miRNA accumulation in shoots and/or roots depending on N availability. On the right, representative conserved miRNAs of the main clusters identified are indicated (for a full

list of the 106 differentially accumulated miRNA isoforms shown in the heatmap, see Supplementary Table S3B). The ratio between the systemic NS response relative to the ND response is shown. The intensity of the differential accumulation is shown with the color scale. (B) Venn diagram highlighting miRNAs regulated in the roots and/or shoots of plants at ND or NS. miR2111 and miR399 are highlighted as they are, respectively, accumulated in both shoots and roots of ND plants, or in both shoots and roots of NS plants. Below the heatmap, graphs show the read numbers from the RNA-seq data for miR399 (left) and miR2111 (right), in shoots or roots of wild-type (WT) or *cra2* mutant plants. (C) Transcript accumulation of a *premiR399* and a *premiR2111* precursor was analyzed by qRT–PCR in shoots and roots of WT or *cra2* mutant plants at ND or NS in the same conditions as for the RNA-seq analysis. Error bars represent the SD. Two independent biological replicates were performed (n>3 plants for each replicate and condition).

Using the previous split-root experimental design (Fig. 1A), small RNA libraries were additionally generated from *cra2* mutant plants. The previously observed accumulation of miR2111 and miR399 isoforms in shoots and systemic roots of ND or NS-treated plants was absent in the *cra2* mutant (Fig. 3B; Supplementary Table S3C). Both families of miRNAs accumulated roughly three to eight times less in the *cra2* mutant compared with the wild-type under control conditions (Supplementary Table S4), in line with previously published results for miR2111 (Gautrat *et al.*, 2021). Accordingly, the expression of a premiR399 precursor was induced in shoots of NS plants depending on CRA2, whereas it was not regulated in roots (Fig. 3C). Conversely, the premiR2111 precursor was induced specifically in shoots of ND plants, in a CRA2-dependent manner, as previously documented (Gautrat *et al.*, 2020). This result further sustains the antagonistic CRA2-dependent systemic regulation of miR399 and miR2111 in shoots by the plant N status. As CEP peptides, notably MtCEP1, act through the CRA2 receptor (Mohd-Radzman *et al.*, 2016; Laffont *et al.*, 2019), we analyzed the involvement of this peptide in the regulation of miR399 by N availability. To this aim, we generated composite *M. truncatula* wild-type plants ectopically expressing *CEP1* in their roots. *CEP1* overexpression slightly affected the accumulation of *premiR399* transcripts in shoots of plants grown under NS, compared with control roots overexpressing *GUS* under the control of the same promoter. However, *CEP1* overexpression had no detectable effect on *PHO2* accumulation in either roots or shoots (Fig. 4A; Supplementary Fig. S3). We hypothesized that the CLE35 signaling peptide, which is induced in response to high nitrate (Moreau *et al.*, 2021), could also act in regulating the N-mediated expression of miR399. *CLE35* overexpression in roots slightly increased miR399 accumulation in shoots, again without affecting *PHO2* transcript accumulation in roots or shoots (Fig. 4B; Supplementary Fig. S3). Overall, these results suggest that CEP and CLE signaling peptides participate in the regulation of the systemic accumulation of miR399 in response to the N status of the whole plant.

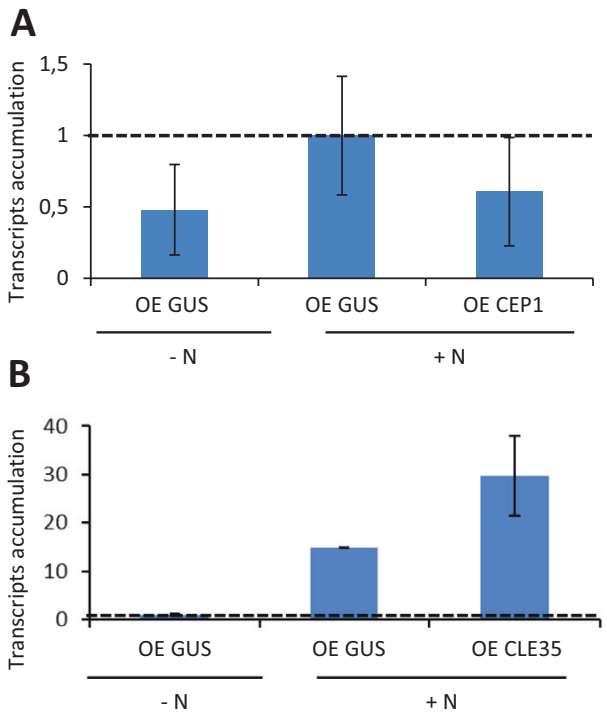

Fig. 4. Impact of MtCEP1 or MtCLE35 signaling peptide overexpression on premiR399 expression. *Medicago truncatula* wild-type plants were transformed with *Agrobacterium rhizogenes* to overexpress in their roots either the MtCEP1 or MtCLE35 signaling peptide. Plants were grown on either low N (–N; KNO_3 0.5 mM) or high N (+N; NH_4NO_3 10 mM) to generate, respectively, a whole-plant N deficiency or N satiety. The transcript accumulation of a *premiR399* precursor in shoots of these composite plants was analyzed by qRT–PCR. (A) Effect of *MtCEP1* overexpression (OE CEP1) compared with a *GUS*-overexpressing control (OE GUS). B. Effect of *MtCLE35* overexpression (OE CLE35) compared with a *GUS*-overexpressing control (OE GUS). Error bars represent the SD. The dotted lines indicate a ratio of 1 relative to the high-N OE GUS control condition in (A) and to the low-N OE GUS control condition in (B). Three independent biological replicates were performed (n>8 plants for each replicate and condition).

Low phosphate availability and miR399 overexpression both inhibit root growth and nodule number

As miR399 was reported to regulate Pi acquisition in *M. truncatula* (Branscheid *et al.*, 2010), we tested the hypothesis that this miRNA could participate in a regulatory mechanism modulating root growth and/or nodulation in relation to Pi availability. Moreover, the observation that the expression of the *premiR399* precursor increased during nodulation (Fig. 5A) suggests a potential role of this miRNA during nodulation. Therefore, we tested the effect of Pi provision and depletion on root growth and nodule formation by growing plants inoculated with rhizobia on medium containing either high Pi

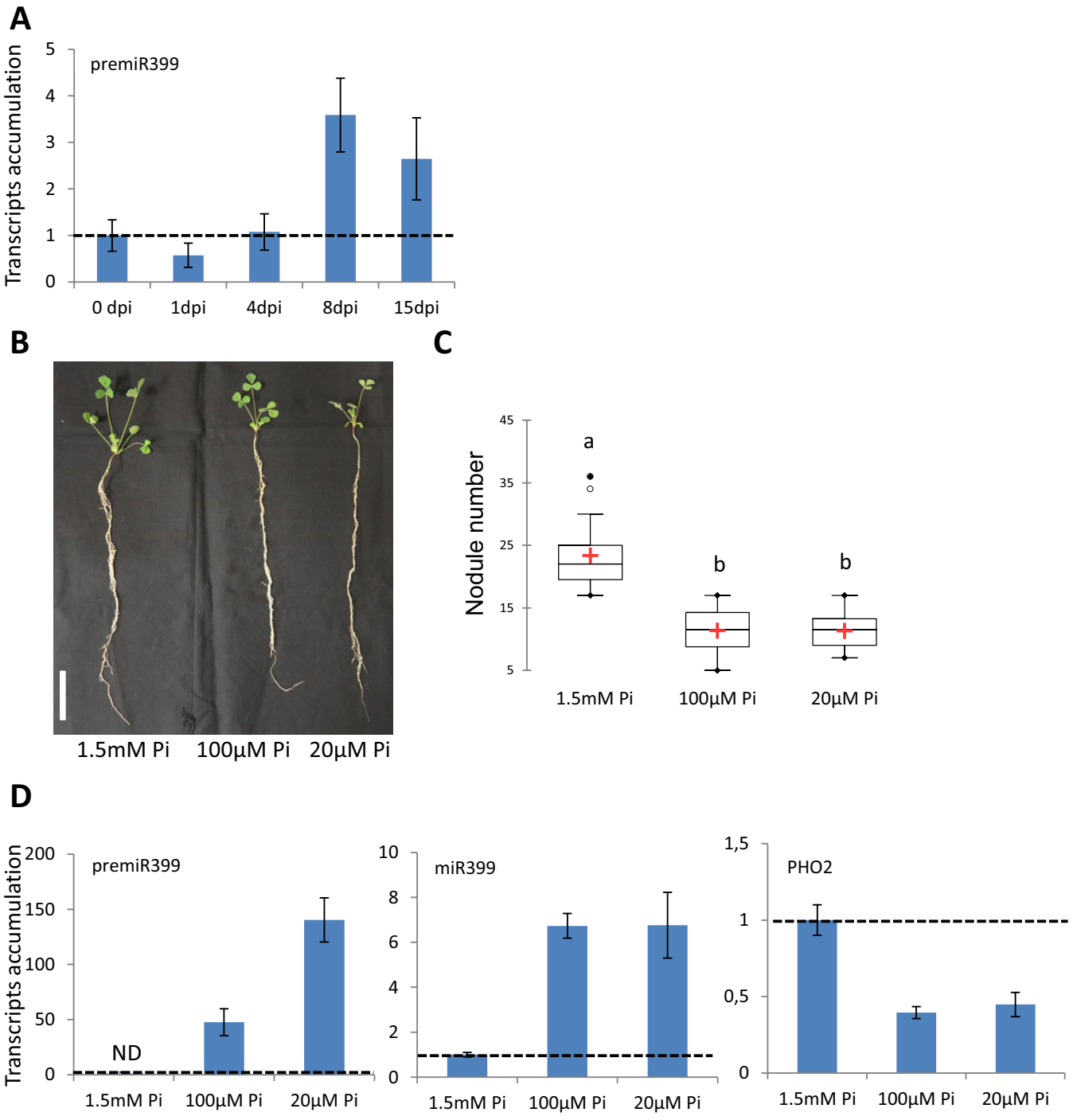

Fig. 5. Impact of inorganic phosphate (Pi) on nodulation and on the accumulation of miR399 and *MtPHO2* transcripts. (A) Expression of a *premiR399* precursor in response to rhizobia, from 0 (non-inoculated roots) to 1, 4, 8, and 15 days post-inoculation (dpi). Transcripts were analyzed by qRT–PCR. Nodules were not visible on roots at 1 dpi and 4 dpi, whereas at 8 dpi root regions with emerging nodules were collected, and at 15 dpi, nodules were collected. Error bars represent the SD. The dotted line indicates a ratio of 1 relative to the 0 dpi control time point. Two biological replicates were performed for each time point. (B, C) Representative image (B) and quantification of nodule number (C) of *M. truncatula* wild-type plants grown on high (1.5 mM) or low (either 100 µM or 20 µM) concentrations of Pi. The center lines show the medians and crosses the means of two independent biological replicates (n=10 plants for each replicate and condition); box limits indicate the 25th and 75th percentiles; whiskers extend to 1.5 times the interquartile range from the 25th and 75th percentiles; outliers are represented by dots. Letters above the plots indicate significant differences based on a Kruskal–Wallis test (α=0.05). (D) Transcript accumulation of a *premiR399* precursor (left), the mature miR399 (middle), and *MtPHO2* target transcripts (right) in roots of *M. truncatula* plants grown in N-satiety conditions (NH_4NO_3 7.5 mM) with high (1.5 mM) or low (either 100 µM or 20 µM) Pi concentrations. Error bars represent the SD; the dotted lines indicate a ratio of 1 relative to the high-Pi condition. Two independent biological replicates were performed (n>8 plants for each replicate and condition). ND, not detected.

(1.5 mM) or low Pi (100 μM or 20 μM). As expected, both of the lower Pi concentrations tested induced miR399 expression, and concomitantly reduced *PHO2* transcript accumulation in roots of plants grown in NS conditions (Fig. 5D). In our experimental set-up, Pi depletion repressed both root growth and nodule formation (Fig. 5B, C; Supplementary Fig. S4). Overall, these results suggest that the regulation of root and nodule development by Pi is antagonistic to the abundance of miR399.

To determine whether the previously identified systemic accumulation of cytokinins in NS plants could be related to the systemic accumulation of miR399 in the NS condition, we analyzed the expression of this miRNA in plants petiole-fed with cytokinin (Supplementary Fig. S5). However, no significant regulation of miR399 or miR2111 expression was observed in these plants. Finally, to assess whether miR399 regulates root and/or nodule development, a *premiR399* overexpression strategy was used to allow the constitutive accumulation of miR399 in *M. truncatula* roots, thus bypassing its regulation by N and Pi availability. The miR399 precursor transgene was efficiently overexpressed in these roots, compared with a *GUS* overexpression control, and conversely, the levels of the *PHO2* target transcripts were reduced (Supplementary Fig. S6). Roots constitutively overexpressing the miR399 transgene formed fewer nodules (Fig. 6A, B) when grown on both high Pi (1.5 mM; Fig. 6A) and low Pi (100 μM; Fig. 6B). The overexpression of miR399 also significantly decreased root dry weight on high Pi (Fig. 6C) but not on low Pi (Fig. 6D). This indicates that the accumulation of miR399 differentially impacts nodules and/or roots depending on the concentration of Pi. However, owing to the impact of miR399 on root growth, we cannot exclude the possibility that the observed nodulation phenotype is indirectly related to the root developmental phenotype.

Discussion

Using a split-root experimental design, we identified candidate shoot-to-root systemic hormonal and miRNA signals based on their simultaneous accumulation in shoots and roots of plants experiencing either ND or NS. A focus on hormones first revealed a coordinated systemic accumulation of the cytokinin *tZ* in both shoots and roots of plants at NS (Fig. 1), as previously reported in different plants, and notably in *A. thaliana* (Poitout *et al.*, 2018). This indicates a likely evolutionary conservation of the cytokinin systemic pathway activated by high N provision. Among all hormonal metabolites tested, none, other than *tZ*, appeared to be a potential systemic signal modulated by N availability. The systemic regulation of *tZ* accumulation in both shoots and roots required the CRA2 signaling pathway. Using a petiole-feeding approach to treat shoots locally with cytokinins resulted in an inhibition of both root biomass and nodulation (Fig. 2). In the model legume *L. japonicus*, iPRPs [N^6-(Δ^2-isopentenyl) adenine riboside 5′-phosphates] cytokinin biosynthesis intermediates were previously shown to accumulate in shoots in response to rhizobia, and local shoot applications through cotyledon feeding systemically inhibited root nodulation (Sasaki *et al.*, 2014). Although the inhibitory effect of cytokinins on nodulation correlates with the accumulation of *tZ* in conditions of mineral N sufficiency that are known to inhibit the symbiotic interaction, the pleiotropic effect observed on root growth does not allow to unambiguously conclude that cytokinins can directly inhibit nodulation.

ABA and JA accumulated in ND plants, but only in shoots (Supplementary Fig. S2). As the concentrations of ABA and JA were very low in roots compared with shoots, this indicates that they are unlikely to act as shoot-to-root systemic effectors. However, ABA and JA could, depending on N availability, regulate other responses in shoots, for example, related to defense and/or abiotic stress tolerance. Indeed, it was shown that N deficiency increases JA accumulation in relation to defense responses in maize (Schmelz *et al.*, 2003), and that N deficiency increases ABA accumulation and the water potential for stomatal closure in cotton (Radin *et al.*, 1982). Finally, despite auxin and SA having well-known functions in nodulation (Stacey *et al.*, 2006; van Noorden *et al.*, 2006), notably in relation to the SUNN systemic pathway in the case of auxin, no difference was observed in the auxin and SA accumulation patterns in relation to N availability.

Besides identifying hormones as candidate shoot-to-root systemic effectors of N-availability responses, we explored miRNA accumulation in shoots and systemic roots of plants grown in a split-root assay (Fig. 3). A total of 47 conserved miRNAs were retrieved, including, notably, miR156, miR398, miR399, and miR2111, which have already been shown to accumulate in the phloem and to act as systemic effectors in different plants (Maizel *et al.*, 2020). Most of these N-regulated miRNAs were, however, differentially accumulated in systemic shoots versus roots. Among these miRNAs, miR156 was reported to affect vegetative phase changes, tuber development in potato, and nodulation in legumes, whereas miR398 was shown to be related to copper starvation (Wang *et al.*, 2015; Maizel *et al.*, 2020). As these miRNAs were differentially or even antagonistically regulated between roots and shoots, they did not display the accumulation profile that would be expected for a shoot-to-root systemic effector regulated in response to N availability. Strikingly, only two miRNA families showed such a coordinated accumulation pattern: miR2111, which accumulated in both shoots and roots of ND plants, and miR399, which accumulated in both shoots and roots of NS plants. The identification of miR2111 is consistent with previous results demonstrating the role of this miRNA in the systemic regulation of nodule and lateral root formation (Tsikou *et al.*, 2018; Gautrat *et al.*, 2020; Moreau *et al.*, 2021; Sexauer *et al.*, 2023), and additionally validates the strategy used for identifying candidate shoot-to-root systemic signals. The other

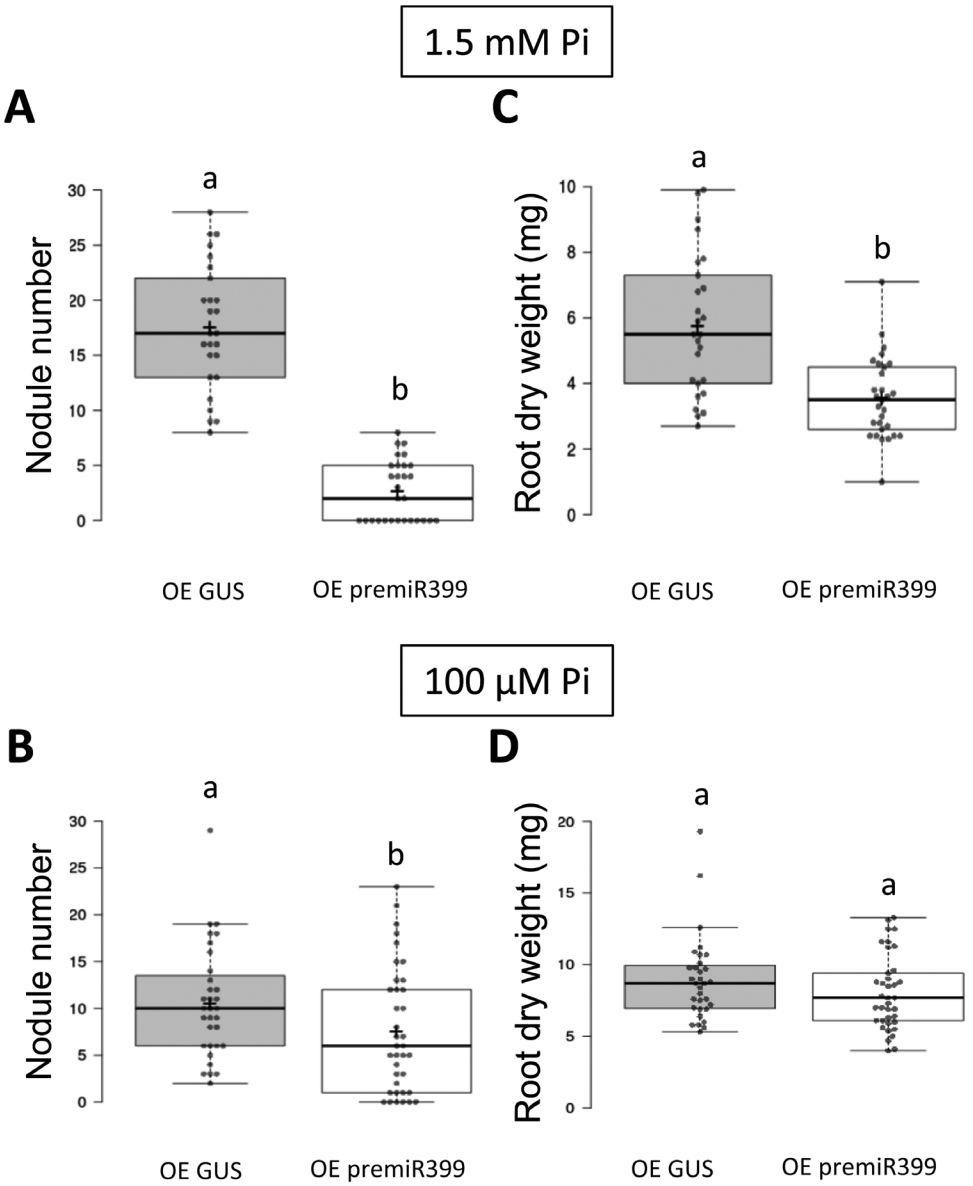

Fig. 6. miR399 reduces root biomass and nodule number. *Medicago truncatula* wild-type plants were transformed with *Agrobacterium rhizogenes* to overexpress the miRNA miR399 in their roots. Plants were grown on Fahraeus medium with either high Pi (1.5 mM) (A, C) or low Pi (100 µM) (B, D). The nodule number was quantified (A, B) as well as the dry weight (C, D) of roots overexpressing a premiR399 (OE premiR399) compared with control OE GUS roots. The center lines show the medians and crosses the means of two independent biological replicates (n>25 plants for each replicate and condition); box limits indicate the 25th and 75th percentiles; whiskers extend to 1.5 times the interquartile range from the 25th and 75th percentiles; individual data points are represented by dots. Letters above the plots indicate significant differences based on a Mann–Whiney U test (α=0.05).

miRNA detected to accumulate simultaneously in both shoots and systemic roots of NS plants was miR399, in agreement with the induction of miR399 accumulation by high nitrate previously documented in Arabidopsis (Medici *et al.*, 2019). This indicates that the crosstalk between Pi and mineral N acquisition through miR399 is likely evolutionarily conserved between Arabidopsis and legumes. The expression of miR399 precursors was detected in both *M. truncatula* shoots and roots, as previously reported (Branscheid *et al.*, 2010), unlike miR2111 precursors, which are specifically expressed in shoots, whereas the mature miR2111 is detected in both shoots and roots as the result of its shoot-to-root mobility (Tsikou *et al.*, 2018; Gautrat *et al.*, 2020). As mature miR399 miRNA was previously detected in phloem sap and was shown by grafting experiments to have a shoot-to-root systemic effect on Pi acquisition (Pant *et al.*, 2008; Branscheid *et al.*, 2010), the identification through the use of a split-root approach of congruent systemic accumulation profiles in both shoots and

roots suggests that a systemic translocation of miR399 may indeed occur in response to NS. Such a systemic action of miR399 from shoots is further supported by the requirement for the CRA2 pathway to allow the miR399 N-dependent differential accumulation in both systemic shoots and roots (Fig. 3). Accordingly, the expression of the premiR399 precursor was similarly systemically differentially regulated by N availability in shoots through the CRA2 pathway. In addition, *MtCEP1* overexpression accordingly reduced miR399 accumulation (Fig. 4), suggesting that MtCEP1, probably together with other CEP peptides, contributes to the systemic regulation of miR399 accumulation depending on N availability. In a related line, the quantification of plant N content and NO_3^- uptake in the *cra2* mutant previously suggested a permanently N-starved phenotype (Bourion *et al.*, 2014; Luo *et al.*, 2023), which is consistent with the observed down-regulation of miR399 in *cra2*. Another candidate long-distance signaling pathway to regulate an miRNA systemically accumulating in NS plants is the MtCLE35 peptide, which was recently shown to mediate the inhibition of nodulation by high N through the miR2111 shoot-to-root systemic effector (Mens *et al.*, 2021; Moreau *et al.*, 2021). An increase of miR399 accumulation was observed upon MtCLE35 overexpression (Fig. 4), suggesting that, similarly as for miR2111 (Gautrat *et al.*, 2020; Moreau *et al.*, 2021), both the CEP and CLE signaling pathways antagonistically regulate miR399 accumulation. This CLE35-mediated up-regulation of miR399 accumulation indicates the involvement of this module in the high-N response, which agrees with the observations in common bean and soybean that Pi deficiency activates the CLE/SUNN systemic pathway to inhibit nodule formation (Isidra-Arellano *et al.*, 2020).

The regulation of miR399 accumulation depending on Pi availability correlates with its impact on the number of nodules formed (Fig. 5). Indeed, as previously shown, low Pi inhibits root nodule formation, promotes miR399 accumulation, and, conversely, reduces the accumulation of *PHO2* transcripts (Branscheid *et al.*, 2010; Sulieman *et al.* 2013). Overexpression of miR399 differentially affects the legume root system architecture depending on the Pi concentration (Fig. 6): at high Pi, reductions in both nodule number and root biomass were evidenced, whereas, at a lower Pi concentration, only the nodule number was affected. This observation indicates that miR399 differentially affects root and nodule development depending on N and Pi availability. However, as previously noted for cytokinins, the effect of miR399 on nodulation may be indirect because of the pleiotropic root growth phenotype, notably observed under high-Pi conditions. The nodulation phenotype of *pho2* mutants was recently analyzed in *M. truncatula* (Huertas *et al.*, 2023). Even though root growth phenotypes were not analyzed, precluding any conclusion about potential indirect effects on nodulation, *PHO2* genes were shown to be required for promoting nodule formation in optimal Pi conditions, and to a lesser extent in low Pi conditions, in agreement with the results now obtained for miR399. The N-availability-dependent regulation of Pi acquisition in plants through the miR399/PHO2 regulatory module is thus likely an evolutionarily conserved feature in plants, which might have been recruited in legumes for regulating symbiotic nodulation. In addition, as miR399 is expressed not only in roots but also in nodules, this suggests that this miRNA might also affect Pi homeostasis inside nodules. Accordingly, in previous studies, Pi levels were shown to be critical for N fixation efficiency (Ma and Chen, 2021), and nodules of *M. truncatula pho2* mutants had a lower biomass and N-fixation capacity (Huertas *et al.*, 2023).

Overall, this study illustrates the tight level of coordination of systemic signaling pathways integrating symbiotic nodulation, root development, and plant N and Pi nutrition. As a perspective, beyond the identification of cytokinins and miR399 as candidate shoot-to-root systemic signals regulating root growth and potentially nodulation in plants at NS, the scope of systemic shoot-to-root molecular cues involved should be expanded, notably to include potential mobile long RNAs, proteins, signaling peptide hormones, and primary and specialized metabolites other than phytohormones.

Supplementary data

The following supplementary data are available at *JXB* online.

Fig. S1. RNA-seq quality control.

Fig. S2. Hormonal analysis of systemic *M. truncatula* shoots and roots depending on N availability.

Fig. S3. Impact of MtCEP1 or MtCLE35 signaling peptide overexpression on *PHO2* expression.

Fig. S4. Impact of Pi availability on *M. truncatula* root dry weight.

Fig. S5. Effect of a cytokinin shoot treatment using petiole feeding on miR399 and miR2111 expression and accumulation.

Fig. S6. Validation of transgene expression in miR399-overexpressing roots.

Table S1. Multiple reaction monitoring (MRM) transitions for all plant hormones analyzed and corresponding internal standards used in this study.

Table S2. Primers used in this study.

Table S3. List of miRNAs differentially accumulated in systemic *M. truncatula* shoots and/or roots depending on N availability.

Table S4. Read numbers of the different miR2111 and miR399 isoforms.

Acknowledgements

Golden Gate cassettes were provided by the 'Engineering the Nitrogen Symbiosis for Africa' (ENSA) project.

Author contributions

FF designed the project; LA, CoM, CaM, MP, ML, CL, and YS performed the experiments; LA, CoM, CaM, MP, CL, YS, TB, ML and FF analyzed and interpreted the results; WK provided the hormonal quantification datasets; HP provided the sRNA libraries and sequencing data; FF wrote the manuscript with contributions from all other authors.

Conflict of interest

The authors declare no competing interests.

Funding

The FF and ML laboratories were the recipient of a collaborative Agence Nationale de la Recherche (ANR) grant (PSYCHE project). The FF laboratory was also funded through the Saclay Plant Sciences (SPS) Labex/EUR, the WK laboratory by a NWO-ENW VIDI (VI.Vidi.193.119) grant, and HP acknowledges financial support from the France Génomique national infrastructure, funded as part of the Investissement d'Avenir program managed by the ANR (ANR-10-INBS-09). We thank the Chinese Academy of Science (CSC) for funding YS.

Data availability

The sRNA-seq data underlying this article are available in in the NCBI Gene Expression Omnibus (GEO) database (https://www.ncbi.nlm.nih.gov/geo/) and can be accessed under accession number GSE247405.

References

Blondon F. 1964. Contribution à l'étude du développement des graminées fourragères ray-grass et dactyle. PhD thesis, Université de Paris, Faculté des Sciences, Paris, France.

Boisson-Dernier A, Chabaud M, Garcia F, Bécard G, Rosenberg C, Barker DG. 2001. *Agrobacterium rhizogenes*-transformed roots of *Medicago truncatula* for the study of nitrogen-fixing and endomycorrhizal symbiotic associations. Molecular Plant-Microbe Interactions **14**, 695–700.

Bourion V, Martin C, de Larambergue H, *et al*. 2014. Unexpectedly low nitrogen acquisition and absence of root architecture adaptation to nitrate supply in a *Medicago truncatula* highly branched root mutant. Journal of Experimental Botany **65**, 2365–2380.

Branscheid A, Sieh D, Pant BD, May P, Devers EA, Elkrog A, Schauser L, Scheible WR, Krajinski F. 2010. Expression pattern suggests a role of miR399 in the regulation of the cellular response to local Pi increase during arbuscular mycorrhizal symbiosis. Molecular Plant-Microbe Interactions **23**, 915–926.

De Kroon H, Visser EJ, Huber H, Mommer L, Hutchings MJ. 2009. A modular concept of plant foraging behaviour: the interplay between local responses and systemic control. Plant, Cell & Environment **32**, 704–712.

Engler C, Marillonnet S. 2014. Golden Gate Cloning. In: Valla S, Lale R, eds. DNA cloning and assembly methods. Methods in Molecular Biology, vol. **1116**. Totowa: Humana Press, 1–24.

Fahraeus G. 1957. The infection of clover root hairs by nodule bacteria studied by a simple glass slide technique. Journal of General Microbiology **16**, 374–381.

Formey D, Sallet E, Lelandais-Brière C, *et al*. 2014. The small RNA diversity from *Medicago truncatula* roots under biotic interactions evidences the environmental plasticity of the miRNAome. Genome Biology **15**, 457.

Gautrat P, Laffont C, Frugier F. 2020. Compact Root Architecture 2 promotes root competence for nodulation through the miR2111 systemic effector. Current Biology: CB **30**, 1339–1345.e3.

Gautrat P, Laffont C, Frugier F, Ruffel S. 2021. Nitrogen systemic signaling: from symbiotic nodulation to root acquisition. Trends in Plant Science **26**, 392–406.

Gautrat P, Mortier V, Laffont C, De Keyser A, Fromentin J, Frugier F, Goormachtig S. 2019. Unraveling new molecular players involved in the autoregulation of nodulation in *Medicago truncatula*. Journal of Experimental Botany **70**, 1407–1417.

Gühl K, Holmer R, Xiao TT, Shen D, Wardhani TAK, Geurts R, van Zeijl A, Kohlen W. 2021. The effect of exogenous nitrate on LCO signalling, cytokinin accumulation, and nodule initiation in *Medicago truncatula*. Genes **12**, 988.

Huertas R, Torres-Jerez I, Curtin SJ, Scheible W, Udvardi M. 2023. *Medicago truncatula PHO2* genes have distinct roles in phosphorus homeostasis and symbiotic nitrogen fixation. Frontiers in Plant Science **14**, 1211107.

Imin N, Mohd-Radzman NA, Ogilvie HA, Djordjevic MA. 2013. The peptide-encoding *CEP1* gene modulates lateral root and nodule numbers in *Medicago truncatula*. Journal of Experimental Botany **64**, 5395–5409.

Isidra-Arellano MC, Pozas-Rodríguez EA, Del Rocío Reyero-Saavedra M, Arroyo-Canales J, Ferrer-Orgaz S, Del Socorro Sánchez-Correa M, Cardenas L, Covarrubias AA, Valdés-López O. 2020. Inhibition of legume nodulation by Pi deficiency is dependent on the autoregulation of nodulation (AON) pathway. The Plant Journal **103**, 1125–1139.

Kozomara A, Birgaoanu M, Griffiths-Jones S. 2019. miRBase: from microRNA sequences to function. Nucleic Acids Research **47**, D155–D162.

Laffont C, Huault E, Gautrat P, Endre G, Kalo P, Bourion V, Duc G, Frugier F. 2019. Independent regulation of symbiotic nodulation by the SUNN negative and CRA2 positive systemic pathways. Plant Physiology **180**, 559–570.

Lepetit M, Brouquisse R. 2023. Control of the rhizobium-legume symbiosis by the plant nitrogen demand is tightly integrated at the whole plant level and requires inter-organ systemic signaling. Frontiers in Plant Science **14**, 1114840.

Love MI, Huber W, Anders S. 2014. Moderated estimation of fold change and dispersion for RNA-seq data with DESeq2. Genome Biology **15**, 550.

Luo Z, Wang J, Li F, *et al*. 2023. The small peptide CEP1 and the NIN-like protein NLP1 regulate *NRT2.1* to mediate root nodule formation across nitrate concentrations. The Plant Cell **35**, 776–794.

Ma Y, Chen R. 2021. Nitrogen and phosphorus signaling and transport during legume–rhizobium symbiosis. Frontiers in Plant Science **12**, 683601.

Maizel A, Markmann K, Timmermans M, Wachter A. 2020. To move or not to move: roles and specificity of plant RNA mobility. Current Opinion in Plant Biology **57**, 52–60.

Martin M. 2011. Cutadapt removes adapter sequences from high-throughput sequencing reads. EMBnet.journal **17**, 10–12.

Medici A, Szponarski W, Dangeville P, *et al*. 2019. Identification of molecular integrators shows that nitrogen actively controls the phosphate starvation response in plants. The Plant Cell **31**, 1171–1184.

Mens C, Hastwell AH, Su H, Gresshoff PM, Mathesius U, Ferguson BJ. 2021. Characterisation of *Medicago truncatula* CLE34 and CLE35 in nitrate and rhizobia regulation of nodulation. New Phytologist **229**, 2525–2534.

Mohd-Radzman NA, Laffont C, Ivanovici A, Patel N, Reid D, Stougaard J, Frugier F, Imin N, Djordjevic MA. 2016. Different pathways act downstream of the CEP peptide receptor CRA2 to regulate lateral root and nodule development. Plant Physiology **171**, 2536–2548.

Moreau C, Gautrat P, Frugier F. 2021. Nitrate-induced CLE35 signaling peptides inhibit nodulation through the SUNN receptor and miR2111 repression. Plant Physiology **185**, 1216–1228.

Okamoto S, Ohnishi E, Sato S, Takahashi H, Nakazono M, Tabata S, Kawaguchi M. 2009. Nod factor/nitrate-induced *CLE* genes that drive

HAR1-mediated systemic regulation of nodulation. Plant & Cell Physiology **50**, 67–77.

Pant BD, Buhtz A, Kehr J, Scheible WR. 2008. MicroRNA399 is a long-distance signal for the regulation of plant phosphate homeostasis. The Plant Journal **53**, 731–738.

Pervent M, Lambert I, Tauzin M, Karouani A, Nigg M, Jardinaud M-F, Severac D, Colella S, Martin-Magniette M-L, Lepetit M. 2021. Systemic control of nodule formation by plant nitrogen demand requires autoregulation-dependent and independent mechanisms. Journal of Experimental Botany **72**, 7942–7956.

Poitout A, Crabos A, Petřík I, Novák O, Krouk G, Lacombe B, Ruffel S. 2018. Responses to systemic nitrogen signaling in Arabidopsis roots involve *trans*-zeatin in shoots. The Plant Cell **30**, 1243–1257.

Prathap V, Kumar A, Maheshwari C, Tyagi A. 2022. Phosphorus homeostasis: acquisition, sensing, and long-distance signaling in plants. Molecular Biology Reports **49**, 8071–8086.

Radin JW, Parker LL, Guinn G. 1982. Water relations of cotton plants under nitrogen deficiency: V. Environmental control of abscisic acid accumulation and stomatal sensitivity to abscisic acid. Plant Physiology **70**, 1066–1070.

Reid DE, Ferguson BJ, Gresshoff PM. 2011. Inoculation- and nitrate-induced CLE peptides of soybean control NARK-dependent nodule formation. Molecular Plant-Microbe Interactions **24**, 606–618.

Roy S, Liu W, Nandety RS, Crook A, Mysore KS, Pislariu CI, Frugoli J, Dickstein R, Udvardi MK. 2020. Celebrating 20 years of genetic discoveries in legume nodulation and symbiotic nitrogen fixation. The Plant Cell **32**, 15–41.

Sakakibara H. 2021. Cytokinin biosynthesis and transport for systemic nitrogen signaling. The Plant Journal **105**, 421–430.

Sasaki T, Suzaki T, Soyano T, Kojima M, Sakakibara H, Kawaguchi M. 2014. Shoot-derived cytokinins systemically regulate root nodulation. Nature Communications **5**, 4983.

Schiessl K, Lilley JLS, Lee T, *et al*. 2019. *NODULE INCEPTION* recruits the lateral root developmental program for symbiotic nodule organogenesis in *Medicago truncatula*. Current Biology **29**, 3657–3668.e5.

Schmelz EA, Alborn HT, Engelberth J, Tumlinson JH. 2003. Nitrogen deficiency increases volicitin-induced volatile emission, jasmonic acid accumulation, and ethylene sensitivity in maize. Plant Physiology **133**, 295–306.

Sexauer M, Bhasin H, Schön M, Roitsch E, Wall C, Herzog U, Markmann K. 2023. A micro RNA mediates shoot control of root branching. Nature Communications **14**, 8083.

Stacey G, McAlvin CB, Kim SY, Olivares J, Soto MJ. 2006. Effects of endogenous salicylic acid on nodulation in the model legumes *Lotus japonicus* and *Medicago truncatula*. Plant Physiology **141**, 1473–1481.

Sulieman S, Ha CV, Schulze J, Tran LS. 2013. Growth and nodulation of symbiotic *Medicago truncatula* at different levels of phosphorus availability. Journal of Experimental Botany **64**, 2701–2712.

Tabata R, Sumida K, Yoshii T, Ohyama K, Shinohara H, Matsubayashi Y. 2014. Perception of root-derived peptides by shoot LRR-RKs mediates systemic N-demand signaling. Science **346**, 343–346.

Tsikou D, Yan Z, Holt DB, Abel NB, Reid DE, Madsen LH, Bhasin H, Sexauer M, Stougaard J, Markmann K. 2018. Systemic control of legume susceptibility to rhizobial infection by a mobile microRNA. Science **362**, 233–236.

Valmas MI, Sexauer M, Markmann K, Tsikou D. 2023. Plants recruit peptides and micro RNAs to regulate nutrient acquisition from soil and symbiosis. Plants **12**, 187.

van Noorden GE, Ross JJ, Reid JB, Rolfe BG, Mathesius U. 2006. Defective long-distance auxin transport regulation in the *Medicago truncatula* super numeric nodules mutant. Plant Physiology **140**, 1494–1506.

Wang Y, Wang Z, Amyot L, Tian L, Xu Z, Gruber MY, Hannoufa A. 2015. Ectopic expression of miR156 represses nodulation and causes morphological and developmental changes in *Lotus japonicus*. Molecular Genetics and Genomics **290**, 471–484.